Universality in bosonic dimer-dimer scattering

A. Deltuva
Centro de Física Nuclear da Universidade de Lisboa, P-1649-003 Lisboa, Portugal
(Received May 16, 2011)

Bosonic dimer-dimer scattering is studied near the unitary limit using momentum-space equations for the four-particle transition operators. The impact of the Efimov effect on the dimer-dimer scattering observables is explored and a number of universal relations is established with high accuracy. The rate for the creation of Efimov trimers via dimer-dimer collisions is calculated.

PACS numbers: 34.50.Cx, 31.15.ac

I. INTRODUCTION

Few-body systems with large two-particle scattering length a possess a number of universal properties that are independent of the short-range interaction details. The three-particle system is simple enough such that analytic or semi-analytic derivation (at least of some) of those properties is possible [1]. Probably the best-known example is the Efimov effect, the existence of an infinite number of weakly bound trimers with geometric spectrum in the unitary limit $a \to \infty$ [2]. The four-particle system, however, is too complicated for analytic approaches and therefore so far has been investigated mostly numerically. While the bound state properties have been calculated by several methods [3–7], the description of the four-particle continuum still constitutes a serious technical challenge, especially in the universal regime with many open channels; first studies have been made using the hyperspherical formalism [8, 9]. Given the success of the four-nucleon scattering calculations [10, 11] based on exact Alt, Grassberger, and Sandhas (AGS) equations [12] that were solved in momentum-space, we applied them recently also to bosonic atom-trimer scattering [13, 14] and established a number of universal relations between observables. In the present work we extend the technique of Ref. [13] to study the universal physics in the bosonic dimer-dimer scattering; in our model only one (shallow) dimer state exists. We note that this problem has already been considered in Ref. [15] using the adiabatic hyperspherical framework. However, the AGS method enables us to determine the universal properties with much higher accuracy; in particular cases there are significant corrections to the results of Ref. [15]. Furthermore, we also present more detailed analysis of dimer-dimer scattering observables.

II. DIMER-DIMER SCATTERING EQUATIONS

A rigorous description of the four-particle scattering can be given by the Faddeev-Yakubovsky equations [16] for the wave-function components or by the equivalent AGS integral equations [12] for the transition operators. The latter ones are better suitable for the multichannel scattering problem where the on-shell momenta and binding energies of the asymptotic states differ by many orders of magnitude [17]. Furthermore, the AGS equations lead more directly to the observables since the on-shell matrix elements of the transition operators calculated between the components of the corresponding initial and final channel states yield scattering amplitudes [18]. For the system of four identical bosons we use the symmetrized form of the AGS equations. In the case of the atom-trimer scattering they are given in Ref. [13], whereas for the dimer-dimer scattering they read

$$\mathcal{U}_{12} = (G_0 t G_0)^{-1} + P_{34} U_1 G_0 t G_0 \mathcal{U}_{12} + U_2 G_0 t G_0 \mathcal{U}_{22}, \tag{1a}$$

$$\mathcal{U}_{22} = (1 + P_{34}) U_1 G_0 t G_0 \mathcal{U}_{12}. \tag{1b}$$

The transition operator $\mathcal{U}_{22}$ describes the elastic scattering and $\mathcal{U}_{12}$ the transfer reactions leading to the final atom-trimer states. The dynamic input is the two-boson potential v. It yields the two-boson transition matrix

$$t = v + v G_0 t \tag{2}$$

and the symmetrized transition operators

$$U_\alpha = P_\alpha G_0^{-1} + P_\alpha t G_0 U_\alpha \tag{3}$$

with $\alpha = 1$ and 2 for the $1+3$ and $2+2$ subsystems, respectively. In the above equations $G_0 = (E + i0 - H_0)^{-1}$ is the free resolvent for the four-boson system with energy E and kinetic energy operator H_0. The permutation operators P_{ij} of particles i and j and their combinations $P_1 = P_{12} P_{23} + P_{13} P_{23}$ and $P_2 = P_{13} P_{24}$ are sufficient to ensure the correct symmetry of the four-boson system when a special choice of the basis states is used [17, 19]. Namely, the basis states must be symmetric under exchange of particles 1 and 2; in addition, for the 2+2 subsystem they must be symmetric also under exchange of particles 3 and 4.

We employ momentum-space partial-wave framework [19] to solve the AGS equations (1). After the discretization of momentum variables the system of integral equations becomes a system of linear algebraic equations whose dimension is significantly reduced by using a separable two-boson potential $v = |g\rangle\lambda\langle g|$ of rank 1 acting in the S wave only. Nevertheless, higher angular momentum states with $l_y, l_z \leq 3$ (see Ref. [19] for the notation) are taken into account for the relative motion in $1+2$,

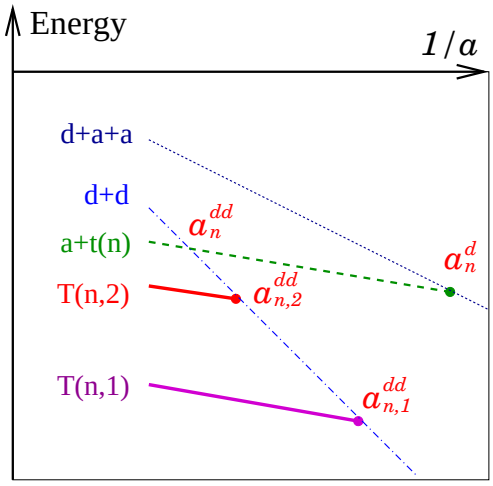

FIG. 1. Schematic representation of the four-boson energy spectrum; only one family (n) of multimers is shown. The tetramer (T) energies, atom-trimer (a+t), dimer-dimer (d+d), and dimer-atom-atom (d+a+a) thresholds are displayed as solid, dashed, dashed-dotted, and dotted lines, respectively. They intersect at special values of a described in the text. For a better visualization only qualitative relations are preserved.

$1+3$, and $2+2$ subsystems such that the results are converged to at least four-digit accuracy with respect to the partial-wave expansion.

To prove that our results are indeed independent of the short-range details of the interaction, we use two different choices of the potential form factor $\langle k|g\rangle = [1+c_2\,(k/\Lambda)^2]e^{-(k/\Lambda)^2}$ with $c_2 = 0$ and $c_2 = -9.17$. It was shown in Ref. [13] that they yield a very different trimer ground state and related observables, but, nevertheless, lead to the same universal relations for the atom collisions with highly excited trimers where the finite-range corrections become negligible.

III. RESULTS

We study the dimer-dimer scattering observables as functions of the atom-atom scattering length a. We fix the geometry of the potential, i.e., the cutoff parameter Λ, whereas the strength λ is adjusted to reproduce the desired value of a. We present the results as dimensionless ratios that are independent of Λ and particle mass m.

A schematic a-dependence of the energy levels and thresholds in the four-boson system is shown in Fig. 1. As a reference point for a we choose the intersection of the dimer-dimer and nth atom-trimer thresholds, i.e., $b_n = 2b_d$ at $a = a_n^{dd}$, where b_d and b_n are the binding energies of the dimer and the nth trimer, respectively. A point important for three-boson physics is $a = a_n^d$ where the nth trimer is at the atom-dimer threshold, i.e., $b_n = b_d$. Furthermore, the existence of two tetramers ($k = 1, 2$) associated with each Efimov trimer was predicted in Refs. [5, 7]. Except for the lowest two, all other tetramers lie above the trimer ground state ($n = 0$) and therefore are unstable bound states [13, 14] with finite width $\Gamma_{n,k}$; their position relative to the four free particle threshold is $-B_{n,k}$. At $a = a_{n,k}^{dd}$ the corresponding tetramer intersects the dimer-dimer threshold, i.e., $B_{n,k} \approx 2b_d$, $\Gamma_{n,k} = 0$, leading to resonant effects in the low-energy dimer-dimer scattering. The relations between these special a values are collected in Table I for $n = 3$ and 4; to achieve the universal limit with good accuracy we concentrate on the regime with n and a large enough, $a\Lambda/2$ ranging from 10^3 to 10^6. The differences between the results obtained with $c_2 = 0$ and $c_2 = -9.17$ in the potential form factor are below 0.3% in the $n = 3$ case and below 0.015% in the $n = 4$ case. In addition we include $a_n^d\sqrt{mb_n^u}$ where b_n^u is the nth trimer binding energy in the unitary limit. The agreement between our predictions and the semi-analytical result $\lim_{n\to\infty} a_n^d\sqrt{mb_n^u} \approx 0.0707645$ given in Ref. [1] is of the same quality as for other ratios in Table I, i.e., it is better than 0.015% in the $n = 4$ case. We therefore conclude that our $n = 4$ calculations provide the universal results for dimer-dimer collisions with high accuracy,

n	$a_{n,1}^{dd}/a_n^{dd}$	$a_{n,2}^{dd}/a_n^{dd}$	a_n^{dd}/a_n^{d}	$a_n^d\sqrt{mb_n^u}$
3	0.32335	0.99948	6.8019	0.070601
4	0.32352	0.99947	6.7896	0.070754
3	0.32369	0.99948	6.7809	0.070857
4	0.32354	0.99947	6.7886	0.070768

TABLE I. Special values of atom-atom scattering length calculated using potential form factor with $c_2 = 0$ (top) and $c_2 = -9.17$ (bottom).

$$a_{n,1}^{dd}/a_n^{dd} = 0.3235(1), \tag{4a}$$
$$a_{n,2}^{dd}/a_n^{dd} = 0.99947(2), \tag{4b}$$
$$a_n^{dd}/a_n^{d} = 6.789(1); \tag{4c}$$

the errors are estimated from the residual dependence on c_2 and included l_y, l_z. The above ratios calculated in Ref. [15] with local potential at $n = 2$ are 0.352, 0.981, and 6.73, respectively. Thus, they differ from our results by 1 to 9%. In particular, our $1-a_{n,2}^{dd}/a_n^{dd}$ value is smaller by a factor of 35, indicating that the shallow tetramer is much closer to the corresponding atom-trimer threshold and thereby much stronger affects the atom-trimer low-energy scattering [14].

In the following we do not demonstrate explicitly the convergence of our results, however, they are checked to be independent of c_2 and n for $n \geq 3$ with good accuracy. In Figs. 2 and 3 we show the dimer-dimer scattering length A_{dd} and the effective range parameter r_{dd} as functions of a. In the universal limit A_{dd}/a and r_{dd}/a are log-periodic functions of a, i.e., the behavior shown

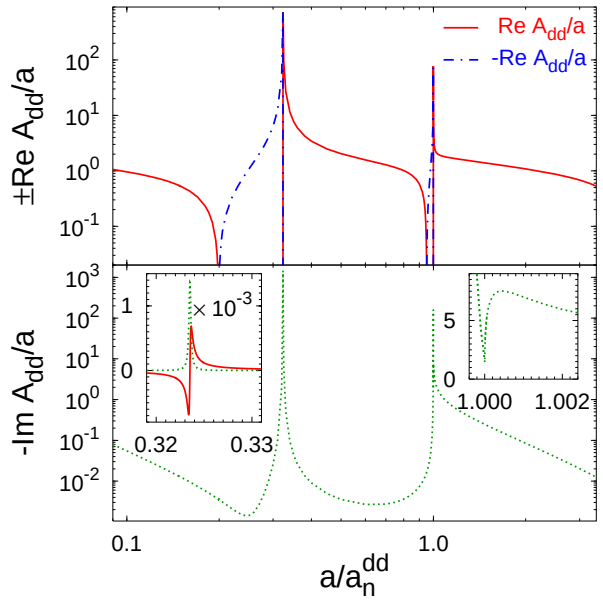

FIG. 2. (Color online) Real and imaginary parts of the dimer-dimer scattering length as functions of the atom-atom scattering length. In the left inset $\mathrm{Re}A_{dd}/a$ (solid curve) and $\mathrm{Im}A_{dd}/a$ (dotted curve) are shown in the vicinity of the $(n,1)$ tetramer using linear scale. In the right inset $\mathrm{Im}A_{dd}/a$ is shown in the vicinity of the dimer-dimer and atom-trimer threshold intersection.

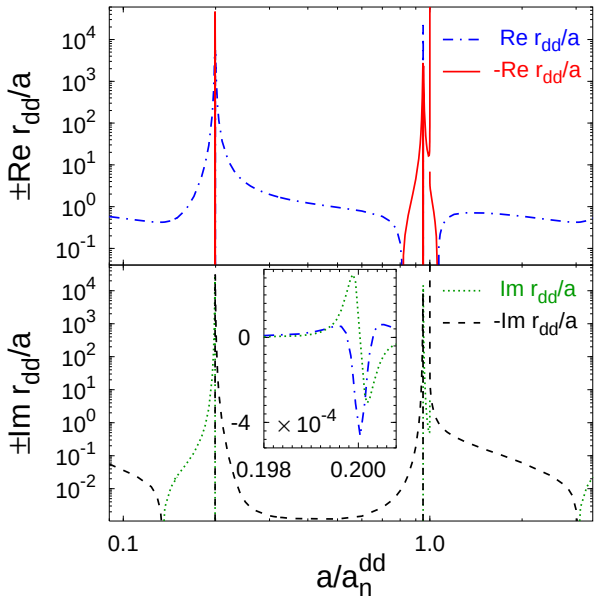

FIG. 3. (Color online) Real and imaginary parts of the dimer-dimer effective range parameter as functions of the atom-atom scattering length. In the inset $\mathrm{Re}\,r_{dd}/a$ (dash-dotted curve) and $\mathrm{Im}\,r_{dd}/a$ (dotted curve) are shown in the vicinity of $\mathrm{Re}A_{dd}=0$ using linear scale.

in Figs. 2 and 3 is repeated when a increases by the Efimov factor $e^{\pi/s_0}\approx 22.694$ [1]. Since A_{dd}/a and r_{dd}/a vary over many orders of magnitude, we use logarithmic scale but distinguish between positive and negative values. A_{dd} exhibits a typical resonant behavior at $a=a^{dd}_{n,k}$; for $k=1$ it is shown with finer resolution in the left inset of Fig. 2. At the intersection of the dimer-dimer and atom-trimer thresholds A_{dd} has a cusp that is especially pronounced for the imaginary part as demonstrated in the right inset of Fig. 2.

The validity region of the effective range expansion is considerably narrower than the difference between the thresholds $|2b_d-b_n|$. Thus, the dimer-dimer effective range parameter r_{dd} is ill-defined at the intersection of the dimer-dimer and atom-trimer thresholds; $\mathrm{Re}\,r_{dd}$ ($\mathrm{Im}\,r_{dd}$) diverges when a approaches a^{dd}_n from below (above) as demonstrated in Fig. 3. In contrast to A_{dd}, r_{dd} shows no resonant feature at $a=a^{dd}_{n,k}$ but exhibits very rapid variations when $\mathrm{Re}A_{dd}$ goes through zero, i.e., at $a/a^{dd}_n\approx 0.200$ and 0.951. In a very narrow region around these a values $\mathrm{Im}\,r_{dd}$ has positive and negative peaks whereas $\mathrm{Re}\,r_{dd}$ has two positive (negative) peaks separated by a much more pronounced negative (positive) peak at $a/a^{dd}_n\approx 0.200$ (0.951); see the inset of Fig. 3. However, despite the dramatic variations of r_{dd}, the quantity $|A^2_{dd}r_{dd}|$ remains almost constant in these regions; this is consistent with the corresponding behavior of the two-particle system [1].

Next we study the dimer-dimer complex phase shifts δ_L and inelasticity parameters $\eta_L=e^{-2\mathrm{Im}\,\delta_L}$ as functions of the relative dimer-dimer energy E_{dd} up to the atom-atom-dimer threshold; L is the orbital angular momentum for the relative dimer-dimer motion. S-wave ($L=0$) results depend strongly on a as shown in Fig. 4 for few specific a values. We remind that the standard effective range expansion is not valid in the case of coinciding thresholds $a/a^{dd}_n=1$. A very rapid decrease of $\mathrm{Re}\,\delta_0$ at $a/a^{dd}_n=1$ is caused by the proximity of the $(n,2)$ unstable tetramer. At $a/a^{dd}_n<1$ the cusp in $\mathrm{Re}\,\delta_0$ and the descent of η_0 correspond to the opening of the nth atom-trimer channel. Due to centrifugal barrier these features are absent in the D wave ($L=2$). $\mathrm{Re}\,\delta_2$ are small but, depending on a, can be of both signs, while η_2 deviate from 1 quite significantly as E_{dd} increases. Thus, near $E_{dd}\approx b_d$ the D-wave contribution to the inelastic cross section may exceed the one of the S wave, the ratio being $5(1-\eta_2^2)/(1-\eta_0^2)$. Higher waves can be neglected in the considered energy regime $E_{dd}<b_d$, i.e., $\delta_L\approx 0$ for $L\geq 4$.

The cross sections for the dimer-dimer elastic scattering $\sigma(dd\to dd)$ and transfer/rearrangement reactions $\sigma(dd\to n')$ leading to an atom plus trimer in the n'th state are shown in Fig. 5. At very low energy $\sigma(dd\to dd)$ become nearly energy-independent (this is true also for $a/a^{dd}_n=1$ at $E_{dd}/b_d<10^{-5}$) while $\sigma(dd\to n')$ increase with decreasing E_{dd} nearly as $E^{-1/2}_{dd}$. The exception is $\sigma(dd\to n)$ in the case of coinciding thresholds $a/a^{dd}_n=1$ where the increase slows down until $\sigma(dd\to n)$ becomes almost constant at $E_{dd}/b_d<10^{-5}$. Thus, the very low energy behavior of the cross sections is consistent with the Wigner threshold law. The reason why for

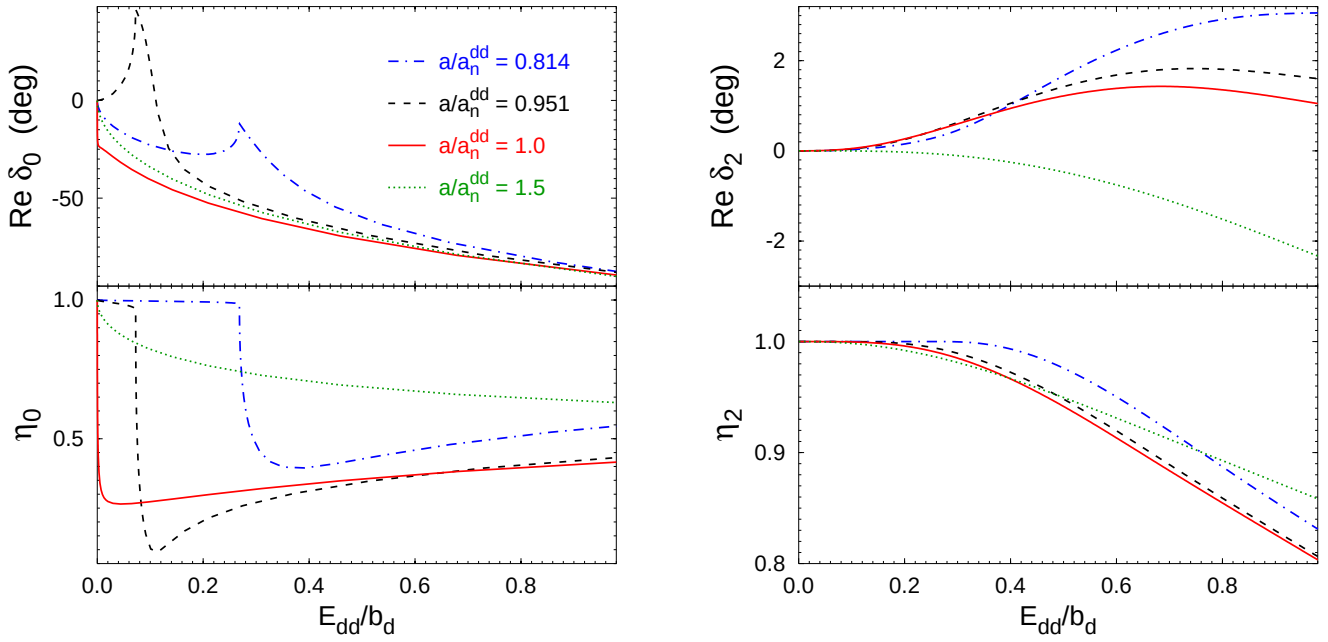

FIG. 4. (Color online) Energy-dependence of the S- and D-wave phase shifts and inelasticity parameters for the dimer-dimer scattering at specified values of the atom-atom scattering length. For a better comparison we set $\mathrm{Re}\,\delta_L = 0$ at $E_{dd} = 0$.

$a/a_n^{dd} = 1$ the region of nearly constant $\sigma(dd \to dd)$ and $\sigma(dd \to n)$ is so narrow is the proximity of the $(n, 2)$ unstable tetramer. The inelastic scattering, apart from the very narrow regions just above the atom-trimer thresholds, is dominated by the open channel with the shallowest trimer; the reactions leading to more deeply bound trimers are strongly suppressed. The elastic cross section appears to be remarkably sensitive to the atom-atom scattering length. For example, $a/a_n^{dd} = 0.814$ corresponds to $\mathrm{Re}\, r_{dd} \approx 0$ leading to an almost constant $\sigma(dd \to dd)$ at $E_{dd}/b_d < 0.1$ while for $a/a_n^{dd} = 0.951$ where $\mathrm{Re}\, A_{dd} \approx 0$ the elastic cross section is very small at $E_{dd} = 0$ but then increases with energy, in contrast to the other shown cases. Furthermore, the opening of the nth atom-trimer channel affects the elastic dimer-dimer cross section in opposite ways for $a/a_n^{dd} = 0.814$ and 0.951.

The above results are indispensable for the description of the dimer-trimer conversion process, i.e., the creation of Efimov trimers via rearrangement reaction in a gas of dimers. The total trimer creation rate in the dimer-dimer scattering $\beta_{dd} = \sum_{n'} \beta_{dd}^{n'}$ has contributions from all open atom-trimer channels,

$$\beta_{dd}^{n'} = \langle v_{dd}\, \sigma(dd \to n') \rangle, \tag{5}$$

where $v_{dd} = \sqrt{2E_{dd}/m}$ is the relative dimer-dimer velocity and $\langle \ldots \rangle$ denotes the thermal average. At vanishing temperature the trimer creation rate $\beta_{dd}(0) = -(8\pi/m)\,\mathrm{Im}A_{dd}$ is determined by the results of Fig. 2; thus, it gets resonantly enhanced around $a = a_{n,k}^{dd}$. The results at finite temperature T, assuming the Boltzmann distribution for the relative dimer-dimer energy, are presented in Fig. 6 for few selected values of a. The shown examples differ remarkably in their T dependence: at very low temperatures β_{dd} decreases with T very rapidly at the resonance ($a/a_n^{dd} = 0.3235$) while in other cases its variation is considerably slower. A more pronounced increase of β_{dd} at higher temperature for $a/a_n^{dd} = 0.814$ and 0.951 is due to the opening of the nth atom-trimer channel. We do not show predictions for individual $\beta_{dd}^{n'}$, but the results of Fig. 5 clearly indicate that shallow trimers are produced most efficiently.

Finally we note that β_{dd} was calculated also in Ref. [15] where it was called the dimer-dimer relaxation rate. There is a good qualitative agreement between our β_{dd} results and those of Ref. [15]. There are, however, some quantitative differences, e.g., at $a/a_n^{dd} = 1.5$ our β_{dd} decreases with T slower. At least to some extent this is probably caused by the significant D-wave contribution taken into account in our calculations.

The only available experimental data [20] refer to the regime where a exceeds the interaction range by a factor 1 to 10 and therefore non-negligible finite-range corrections can be expected. In this respect our calculations present no improvement over those of Ref. [15] that could provide only qualitative explanation of some features of the data. However, our predictions would be valuable for the future experiments performed in the universal regime.

IV. SUMMARY

We studied bosonic dimer-dimer scattering near the unitary limit. It is a complicated multichannel four-

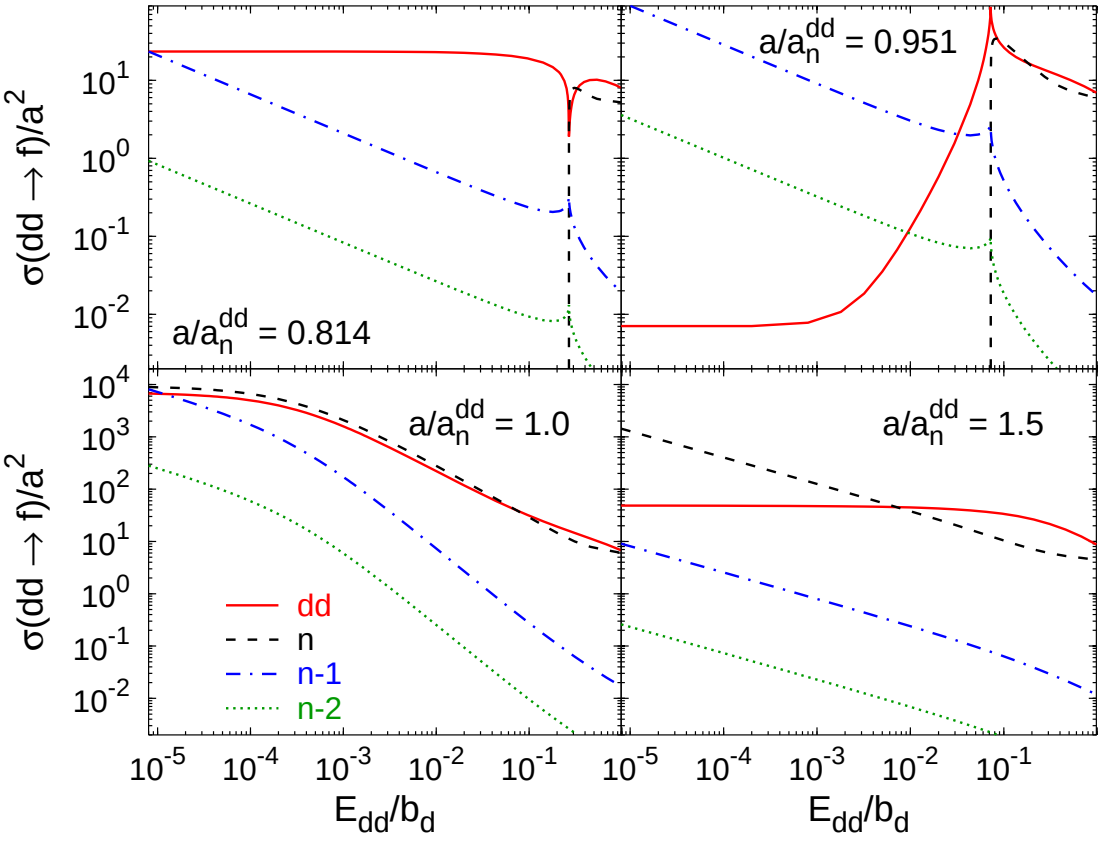

FIG. 5. (Color online) Elastic and transfer cross sections for the dimer-dimer scattering at specified values of the atom-atom scattering length.

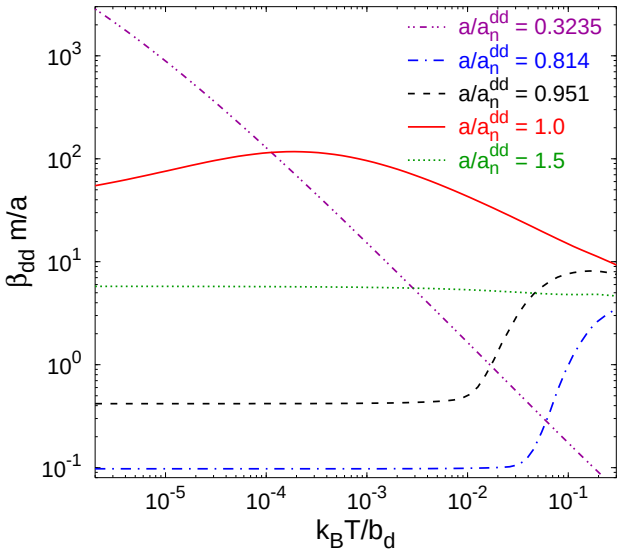

FIG. 6. (Color online) Temperature dependence of the trimer creation rate at specified values of the atom-atom scattering length; $a/a_n^{dd} = 0.3235$ corresponds to the $(n,1)$st resonance that leads to a peak of β_{dd} at $T = 0$.

particle scattering problem involving, in the present calculations, one dimer-dimer and up to five atom-trimer channels with very broad range of binding energies. Exact AGS equations were solved using momentum-space techniques. The log-periodic structure of the dimer-dimer scattering observables was found to be independent of the short-range potential details. Universal results for the dimer-dimer scattering length, effective range, phase shifts, elastic and transfer cross sections, some tetramer properties, and trimer creation rate were obtained with an accuracy considerably higher than in previous works.

[1] E. Braaten and H.-W. Hammer, Phys. Rep. **428**, 259 (2006).

[2] V. Efimov, Phys. Lett. B **33**, 563 (1970).

[3] D. Blume and C. H. Greene, J. Chem. Phys. **112**, 8053 (2000).

[4] L. Platter, H. W. Hammer, and U.-G. Meißner, Phys. Rev. A **70**, 052101 (2004).

[5] H. W. Hammer and L. Platter, Eur. Phys. J. A **32**, 113 (2007).

[6] R. Lazauskas and J. Carbonell, Phys. Rev. A **73**, 062717 (2006).

[7] J. von Stecher, J. P. D'Incao, and C. H. Greene, Nature Phys. **5**, 417 (2009).

[8] J. P. D'Incao, S. T. Rittenhouse, N. P. Mehta, and C. H. Greene, Phys. Rev. A **79**, 030501(R) (2009).

[9] Y. Wang and B. D. Esry, Phys. Rev. Lett. **102**, 133201 (2009).

[10] A. Deltuva and A. C. Fonseca, Phys. Rev. Lett. **98**, 162502 (2007); Phys. Rev. C **81**, 054002 (2010).

[11] A. Deltuva, A. C. Fonseca, and P. U. Sauer, Phys. Lett. B **660**, 471 (2008).

[12] P. Grassberger and W. Sandhas, Nucl. Phys. **B2**, 181 (1967); E. O. Alt, P. Grassberger, and W. Sandhas, JINR report No. E4-6688 (1972).

[13] A. Deltuva, Phys. Rev. A **82**, 040701(R) (2010).

[14] A. Deltuva, arXiv:1103.2107 (2011).

[15] J. P. D'Incao, J. von Stecher, and C. H. Greene, Phys. Rev. Lett. **103**, 033004 (2009).

[16] O. A. Yakubovsky, Yad. Fiz. **5**, 1312 (1967) [Sov. J. Nucl. Phys. **5**, 937 (1967)].

[17] A. Deltuva, R. Lazauskas, and L. Platter, Few-Body Syst., accepted for publication.

[18] A. Deltuva and A. C. Fonseca, Phys. Rev. C **76**, 021001(R) (2007).

[19] A. Deltuva and A. C. Fonseca, Phys. Rev. C **75**, 014005 (2007).

[20] F. Ferlaino *et al.*, Phys. Rev. Lett. **101**, 023201 (2008).

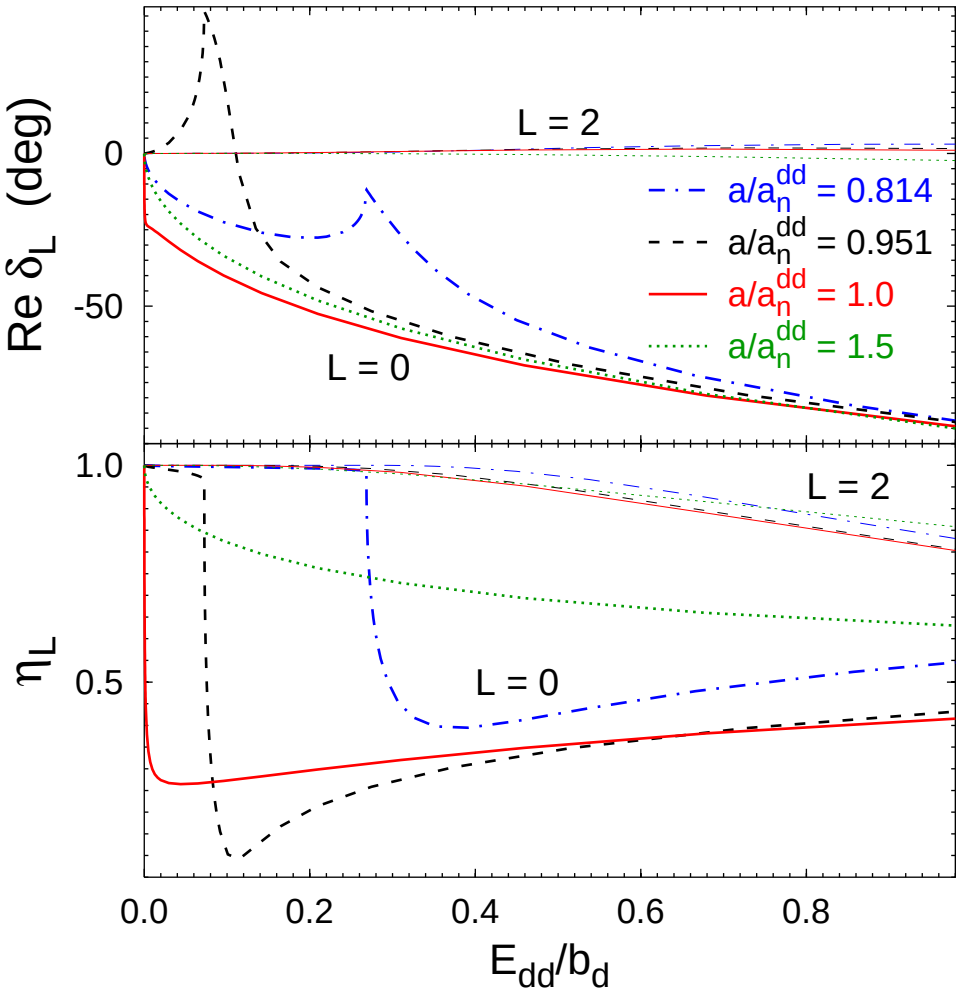
Re δ_L (deg)
0
-50
L = 2
L = 0
a/a_n^dd = 0.814
a/a_n^dd = 0.951
a/a_n^dd = 1.0
a/a_n^dd = 1.5
η_L
1.0
0.5
L = 2
L = 0
0.0
0.2
0.4
0.6
0.8
E_dd/b_d